Consequences of Magnesium in 5050 Aluminum Alloy on Wettability, Strengthening Mechanisms and Fracture Behavior of Silicon Carbide Nanoparticle Metal Matrix Composites

A. Chennakesava Reddy
Dept. of Mechanical Engineering, JNT University, Hyderabad, Telangana, India

Abstract
Very recently, the use of 5050 Al alloy has been tremendously increased in the navy and aerospace industries because of its excellent corrosion resistance even in salt water and very high toughness even at cryogenic temperatures. This work was attempted to estimate the effect magnesium content in 5050 Al alloy on the improvement of wettability, tensile strength and elastic modulus of SiC/5050 Al alloy composites cast by stir casting route. The wettability, strength, and modulus of elasticity were improved due to increase of wettability. The other mechanisms, which could enhance properties of SiC/5050 Al alloy composites, were grain boundary strengthening and precipitation strengthening.

Keywords
5050 Al Alloy, Magnesium, Silicon Carbide, Strengthening Mechanisms, Fracture Behavior

I. Introduction

Metal Matrix Composites [MMC] with high specific stiffness and strength are employed in applications in which saving weight is a chief issue [1]. The reinforcement is very significant because it governs the mechanical properties, cost and performance of a given composite. Two types of discontinuous reinforcement are used for MMCs: particulate and whiskers. Whiskers generally cost more than particulate reinforcements. For instance, silicon carbide whiskers cost ₹13000 per kg, whereas silicon carbide particulates cost ₹436 per kg. The first production application of a particulate reinforced MMC in the United States was a set of covers for a missile guidance system.

The stiffness and strength of particulate reinforced aluminum MMCs are significantly better than those of the aluminum matrix. For instance, at a volume fraction of 30% silicon carbide particulate reinforcement, the strength is about 45 percent greater than that of the 6061 Al alloy matrix and the stiffness is doubled [2-3]. Silicon carbide (SiC) nanoparticles possess high thermal conductivity, low thermal expansion coefficient and good wear resistance. Silicon carbide nanoparticles are especially used high-temperature ceramic bearings, sealing valves and spray nozzles. The main issue of SiC nanoparticles is the low wettability by the molten metal. Exclusively, the conventional casting processes yield in inhomogeneous distribution of particles within the matrix. Also, the high surface energy of nanoparticles motivates to form clusters, which are inadequate to block the movement of dislocations for the strengthening of composites.

Aluminum alloys such as 1xxx [4], 2xxx [5], 3xxx [6], 4xxx [7], 5xxx [8], 6xxx [9], 7xxx [10] and 8xxx [11] have been used with several reinforced nanoparticles. The SiC particles were reinforced with Al alloys such as pure Al [12], 2024 Al alloy [13], 6063 Al alloy [14, 15], 7020 Al alloy [16, 17] and 8090 Al alloy [18], as yet 5050 Al alloy is not used with SiC nanoparticles. The 5xxx series of Al alloys are strain hardenable; have moderately high strength, excellent corrosion resistance even in salt water; and very high toughness even at cryogenic temperatures. Several researchers [19-22] have employed chemically activated wetting method to produce aluminum matrix composite reinforced with ceramic particles. They conveyed that Mg, Ca, Ti, Si, Zr and Zn could be selected as a wetting agent to ease the integration of ceramic particles by molten aluminum. Till date, Magnesium (Mg) is used to enhance solid solution hardening and strain hardening of 5050 Al alloy.

The wetting of the silicon carbide (SiC) nanoparticles by molten aluminum (Al) alloy is essential to the formation of beneficial metal matrix composites. To accomplish this, Mg alloying of aluminum has been expected to increase the wetting of the alloy on the SiC nanoparticles. The present investigation aims at fabricating of SiC/5050 Al alloy composites and to admit the improvement of strength, stiffness and fracture behavior by increasing the wettability of SiC nanoparticles with molten 5050 Al-alloy thorough the addition of Mg.

II. Materials and Methods

The raw materials are 99% pure aluminum, 99% pure magnesium, SiC nanoparticles of 100 nm size as shown in fig. 1. The magnesium content was varied from 2.0% to 3.0% in 99% pure aluminum to get the composition of 5050 Al alloy. The melting practice was carried in the resistance furnace as per standards. The composite, with 30 vol.% SiC content, was produced by the stir casting and low-pressure die casting process. The cast composites were given H32 heat treatment. The flat-rectangular tensile specimens used in the work is shown in figure 2(a) & 2(b). Tensile tests were conducted on a Universal Testing Machine (UTM) with across load speed of 0.5 mm/min at room temperature (ASTM D3039).

The fractured surfaces of the test samples were analyzed with a scanning electron microscope (SEM) using S-3000N Toshiba SEM. Drop Shape Analysis (DSA) was also carried for determining the spread angle. A drop of 5050 Al alloy at 700°C was metered onto a 10.0 mm dia. silicon carbide spherical ball. The drop shape and spread angle was analyzed using profile projector.

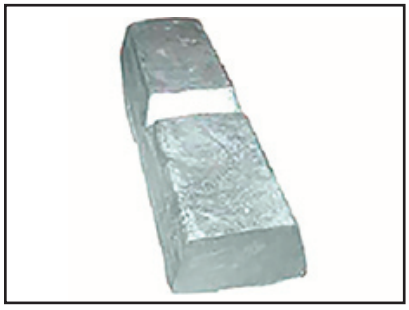

(a)

ISSN : 2249-5762 (Online) | ISSN : 2249-5770 (Print)

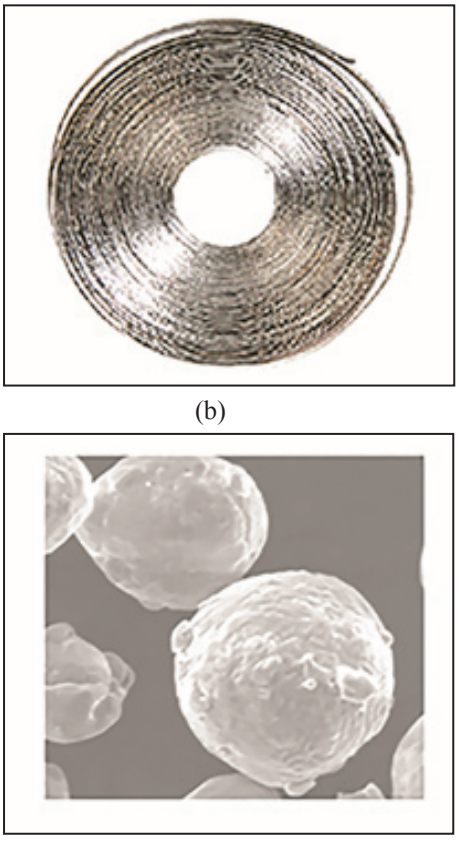

(b)

(c)

Fig. 1: Raw Materials Used in the Present Work: 99% Pure Al, (b) 99% Pure Mg and (c) SiC Nanoparticles.

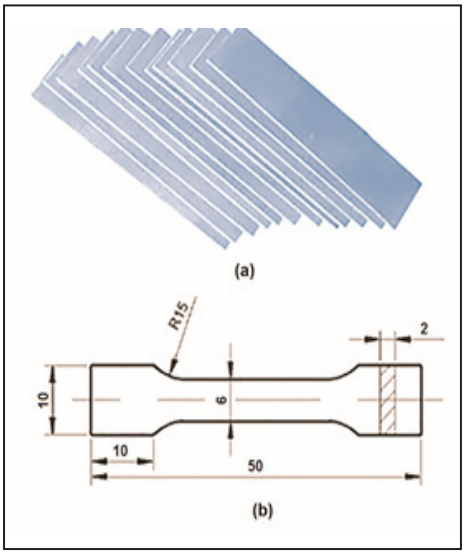

Fig. 2: As-cast SiC/5050 Al Alloy Composites (a) 2mm Thick Specimens for Tensile Tests and (b) Shape and Dimensions of Tensile Specimen (mm).

III. Results and Discussion

In the present work, the Mg content was limited to 3.0% only, because the magnesium would form MgO precipitates beyond 3.0% in 5050 Al alloy. The formation MgO precipitates is seen in figure 3 representing the 5050 Al alloy consisting of 4.0% Mg. The SiC nanoparticles were found randomly distributed (fig. 4) in the 5050 Al alloy matrix. Micro voids between the clusters were also seen in the microstructures of the SiC/5050 Al alloy composites. At places, the clusters (fig. 5) of SiC nanoparticles were observed in the SiC/5050 Al alloy composites.

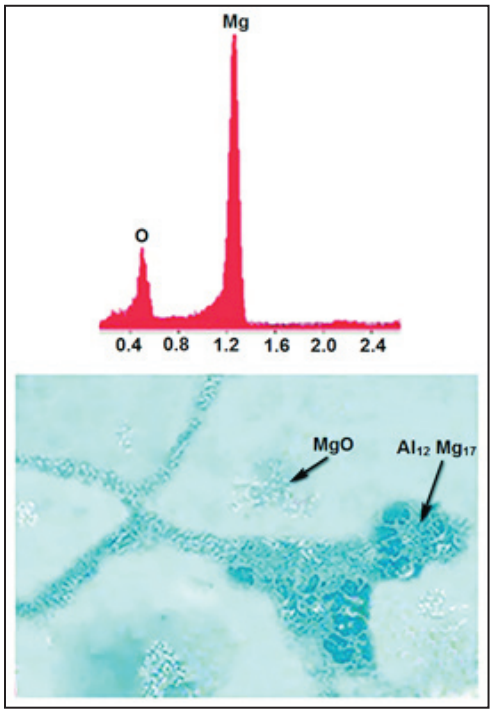

Fig. 3: Formation of MgO in 5050 Al alloy.

A. Analysis of Wettability

Drop Shape Analysis (DSA) is an image analysis method for determining the spread angle. In the present work, the spread angle is an included angle measured between the edges of meatal in contact with the SiC spherical ball. As shown in figure 6, the spreading of 5050 Al alloy on the SiC spherical ball increases with an increase in Mg content in 5050 Al alloy. Consequently, the wettability of SiC nanoparticles increases with an increase in Mg content in 5050 Al alloy. Also, the chemical reaction between these materials promotes the wettability. The DSA shows that the interfacial reaction increases the spread angle from 100° to 123° for the change of Mg content from 2.0% to 3.0%.

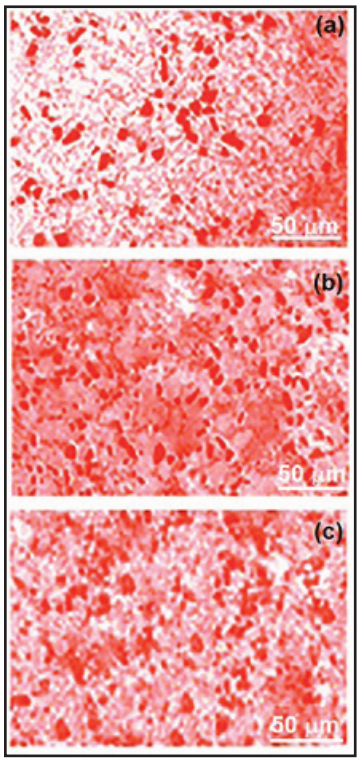

Fig. 4: Microstructures of SiC/5050 Al Alloy Composites: (a) 2.0%Mg, (b) 2.5%Mg and (c) 3.0%Mg.

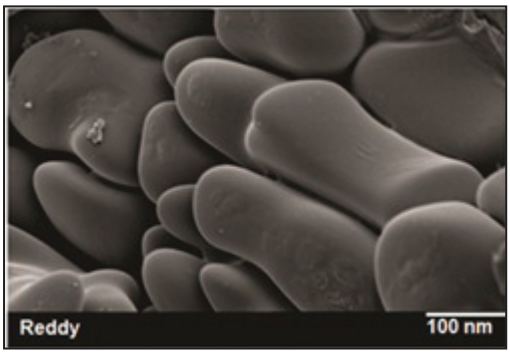

Fig. 5: Formation of Clusters in SiC/5050 Al Alloy Composite

Geometrically, the contact angle can be computed by measuring the droplet diameter and the height of the apex as shown in fig. 7. The contact angle (θ) is, thus, calculated using the following relation:

$$\frac{\theta}{2} = tan^{-1}\left(\frac{h}{d}\right) \quad (1)$$

Work of adhesion, $\frac{\theta}{2} = tan^{-1}\left(\frac{h}{d}\right)$ (2)

Interfacial energy, $\gamma_{pm} = \gamma_p + \gamma_m - W_A$ (3)

Spreading coefficient, $S_c = \gamma_p - \gamma_m - \gamma_{sl}$ (4)

where, γm and γp are, respectively, the surface energies of matrix and particulate materials. The contact angles were, respectively, 61.3o, 57.0o and 50.6o for Mg content of 0.2%, 0.25% and 0.3% in 5050 Al alloy. The contact angles found in the present work were within the acceptable range as compared with another work [23], wherein the contact angle for SiC/Al composite was found to be θ <90°.

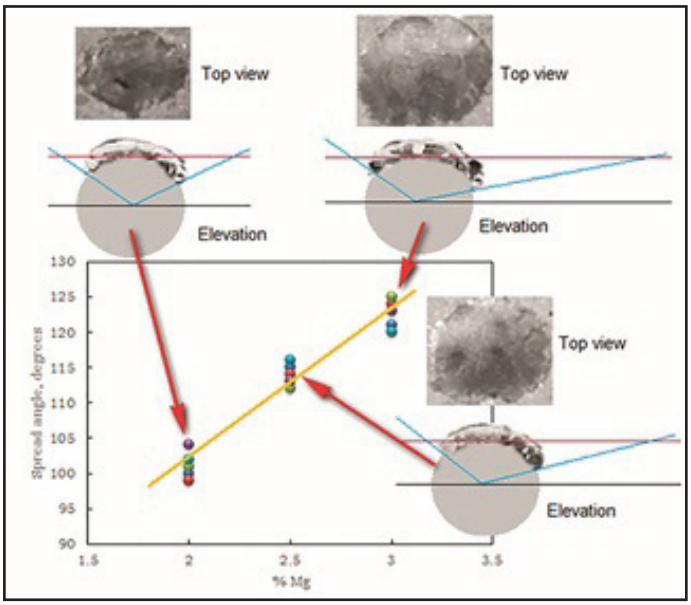

Fig. 6: Drop Shape Analysis of 5050 Al Alloy on SiC Spherical Ball

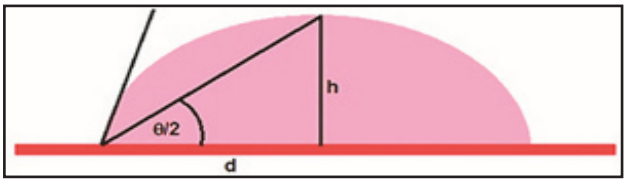

Fig. 7: Determination of Contact Angle

Wetting of nanoparticles and adhesion between nanoparticle and matrix is governed by the principles of theory of adhesion based on the surface energy properties of nanoparticle and matrix, respectively. For the SiC nanoparticles, the surface area does not change without affecting its chemical potential. As shown in figure 8, the work of adhesion increases with a decrease in the contact angle. Also, the SiC nanoparticle encourages the higher work of adhesion due to its high surface energy. The work of adhesion, which is the work required to separate the SiC nanoparticle and the matrix 5050 Al alloy, increases with Mg concentration. As described in [24], the work of adhesion decreases as the interfacial bonding is decreased.

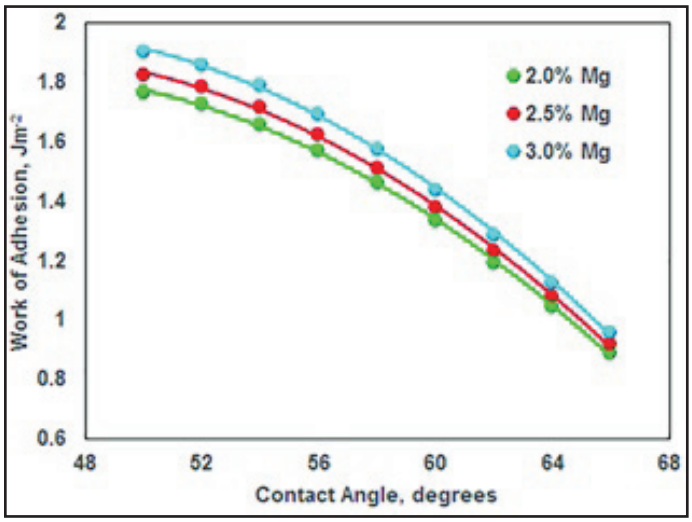

Fig. 8: Effect of Contact Angle on the Work of Adhesion.

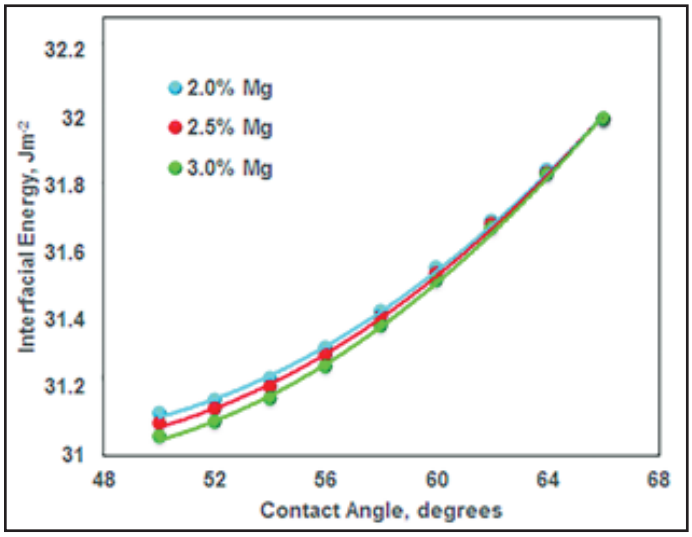

Fig. 9: Effect of Contact Angle on the Interfacial Energy.

The interfacial energy is defined as the energy needed to form a unit area of the new interface between nanoparticle and matrix. This is always less than the sum of surface energies of the two phases (nanoparticle and the matrix) owing to the existence of some energy of attraction between nanoparticle and matrix. To form an interface between SiC nanoparticle and matrix 5050 Al alloy, the required internal energy decreases with an increase in the concentration of Mg as shown in fig. 9. There is lack of spontaneous wetting between the SiC nanoparticle and matrix 5050 Al alloy as the values of spreading coefficient are negative as shown in fig. 10. This means that the bonding between the SiC nanoparticle and the matrix 5050 Al alloy is imperfect (implies to partial bonding).

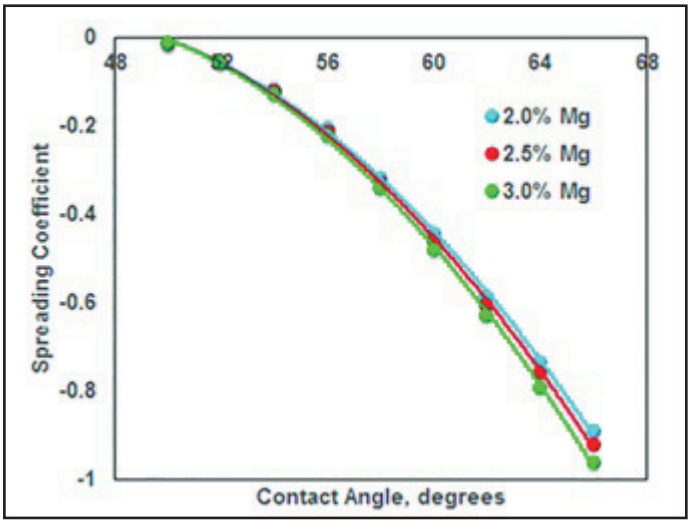

Fig. 10: Effect of Contact Angle on the Spreading Coefficient

B. Schemes for Composite Strength

The particulate nanocomposites contain reinforcing particles in nanoscale (≤100 nm). The issues, that perform key roles in the properties of nanocomposites, are nanoparticle-matrix interaction and particle-particle interaction. The nanoparticle-matrix interaction represents the wettability and adhesiveness. The particle-particle interaction characterizes the formation of nanoparticle clusters. The attraction forces between nanoparticles, due to the van der Waals and electrostatic forces, affect the particle-particle interaction and deteriorate the composite's performances [25]. The quality of interface and the strength of adhesion at the interface determine load transfer between the matrix and the nanofillers [26]. In the literature, available to till date, different formulae were applied to estimate adhesion between matrix and nanoparticles. As shown in fig. 11, the tensile strength increases with increasing content of Mg content in 5050 Al alloy which was used to fabricate SiC/5050 Al alloy composites.

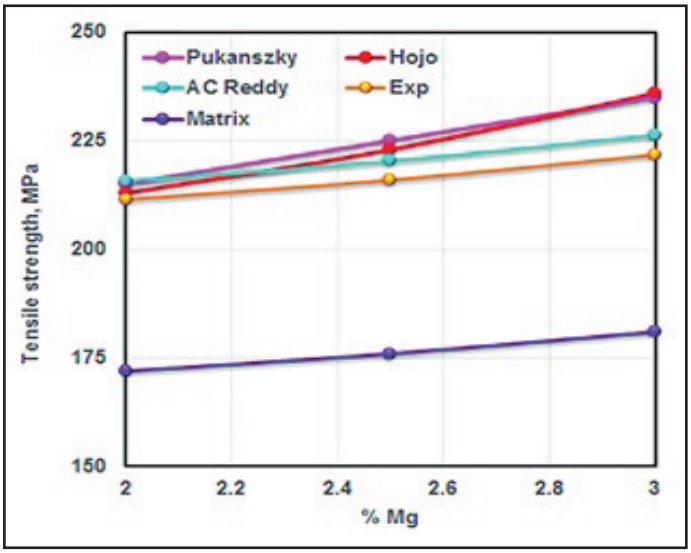

Fig. 11: Tensile Strength of SiC/5050 Al Alloy Composites as a Function of Magnesium Content

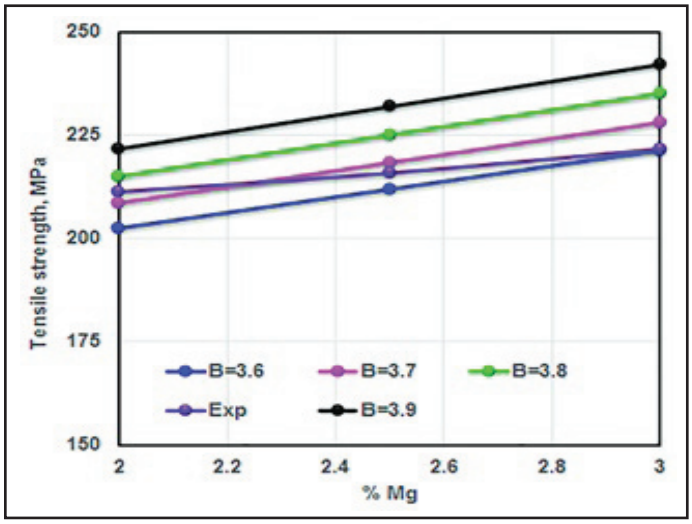

Fig. 12: Effect of Empirical Constant on Strength of SiC/5050 Al Alloy Composites for Expression Proposed by Pukanszky et al.

Pukanszky et al. [27] gave an empirical relationship to find the composite strength with strong particle–matrix interfacial bonding as mentioned below:

$$\sigma_c = \left[\frac{1-v_p}{1+2.5v_p}\sigma_m\right] exp(Bv_p) \quad (5)$$

where B is an empirical constant, which depends on the surface area of particles, particle density and interfacial bonding energy. The composite strength was determined for the range of B varying from 3.6 to 3.9. The experimental values fit only for the value of B between 3.7 and 3.8 at lower concentrations of Mg as shown in fig. 12.

Hojo et al. [28] predicted the composite strength considering the mean particle size dp according to the relation:

$$\sigma_c = \sigma_m + k(v_p) d_p^{-1/2} \quad (6)$$

where $k_p(vp)$ is a constant being a function of the particle loading; k_p is relative change in strength of matrix due to the presence of the particulate. The values of k_p were 0.41, 0.43 and 0.48, respectively, for the Mg concentrations of 2.0%, 2.5% and 3.0% in aluminum as obtained from the tensile strength plots. Even though, the results coincide with the test results for low concentrations of Mg, but this scheme fails for high concentrations of Mg higher than 2.5%.

Considering adhesion, formation of precipitates, particle size, agglomeration, voids/porosity, obstacles to dislocations and interfacial reaction between particle and matrix, a criterion was proposed for the strength of composite [29-30] as given below:

$$\sigma_c = \left[\frac{1-v_p}{1+2.5v_p}\sigma_m\right] exp(Bv_p) \quad (7)$$

$$k = E_m m_m / E_p m_p$$

where v_v and v_p are the volume fractions of voids and the nanoparticle in the composite, mm and mp are the possion's ratios of the matrix and nanoparticless and dp is the mean diameter of the nanoparticle. The results obtained from this model were within the acceptable limit (2%) of the experimental values. The experimental values of tensile strength were lower than the strength values predicted from this model due to partial bonding between the SiC nanoparticles and the matrix 5050 Al alloy.

It can be seen form figure 13 that the high-angle grain boundaries are found in the matrix 5050 Al alloy encouraging a high density of dislocations. High-angle grain boundaries (large misorientation angles) are effective in blocking the dislocations. The yield and tensile strengths rest on the ease with which dislocations can move. Increasing the dislocation density enhances the tensile strength which compels for the requirement of a higher shear stress to move the dislocations. When the dislocations gather progressively at the grain boundary, sub-grain boundaries can form due to the stress concentration at the tip of the leading dislocation as shown in fig. 14.

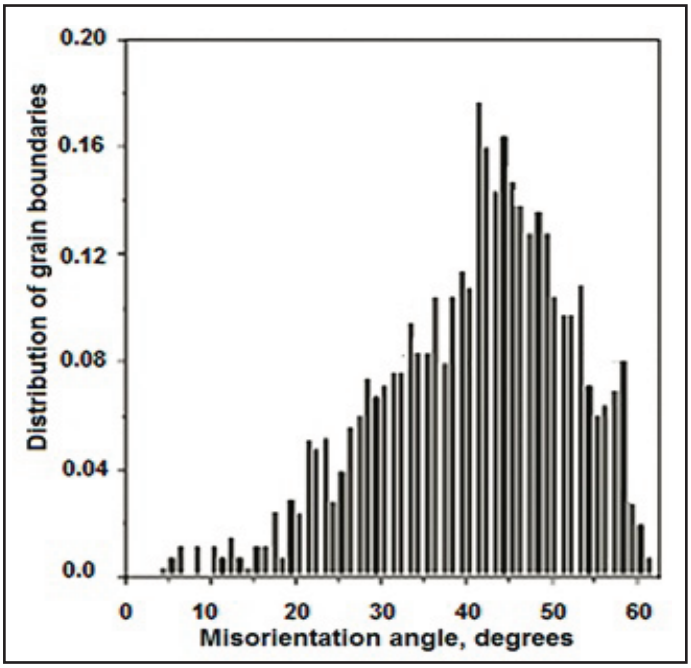

Fig. 13: Misorientation Angles of Grain Boundaries

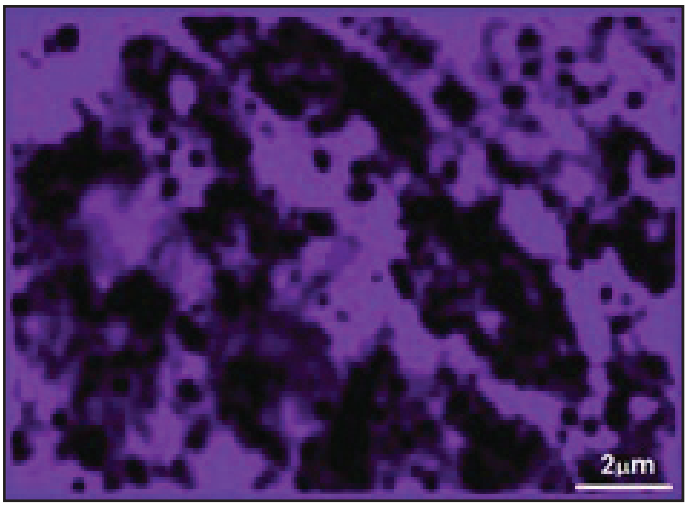

Fig. 14: Formation of Sub-Grains in 5050 Al Alloy

As the volume fraction of SiC nanoparticles was increased in 5050 Al alloy (matrix), the clustering tendency was increased. Consequently, the reduction of load transfer from the matrix to the SiC nanoparticles as seen from fig. 15. The schemes of Pukanszky et al. [27] and Hojo et al. [28] did not consider the formation of clusters; therefore, they are not applicable to the nanocomposites wherein the nanoparticles tend to form clusters. The scheme proposed by AC Reddy [29-30] could reflect the loss of strength due to the formation of clusters as the results express the similar trend of experimental results as shown in fig. 15.

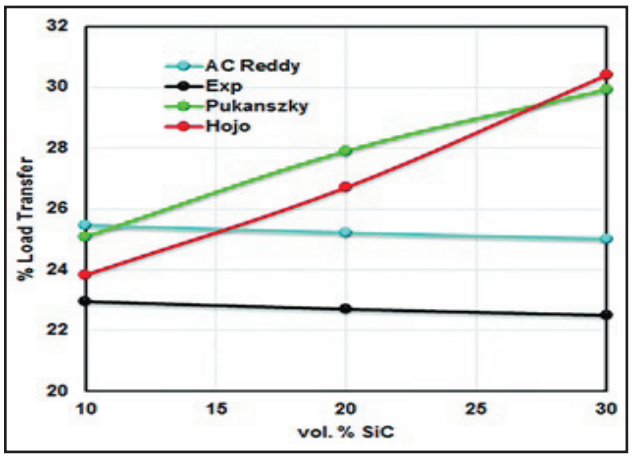

Fig. 15: Load Transfer in SiC/5050 Al Alloy Composites

As shown in Al-Mg phase diagram (fig. 16), the maximum solubility of Mg in Al is 17.4%. As per the binary phase diagram of Al-Mg, the strengthening precipitates could be α, β (Al_3Mg_2) and γ ($Al_{12}Mg_{17}$) phases. As 5050 Al alloy consists of considerable amount of Si, there is a possibility of Al-Si-Mg ternary phase diagrams. From the Al-Si-Mg ternary phase diagram (fig. 17), the probable strengthening precipitate could be Mg_2Si. Also, the condensation of surplus vacancies into dislocation loops helps the nucleation Si clusters. Diamond structure (A4) is formed from Si precipitates without intermediate stages from the Si clusters. Figure 18 reveals the formation of strengthening precipitates in 5050 Al alloy. The β phase was present in the three studied samples. The γ phase was noticed in the 5050 Al alloy consisting of 0.30% Mg. An increase in the composite strength can also be attributed to the precipitate strengthening.

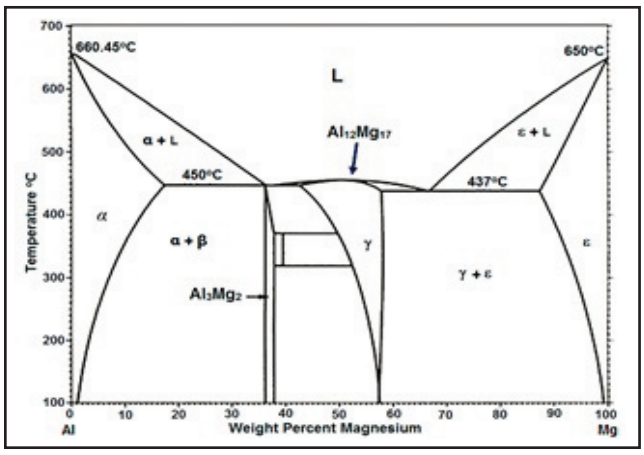

Fig. 16: Al-Mg Phase Diagram

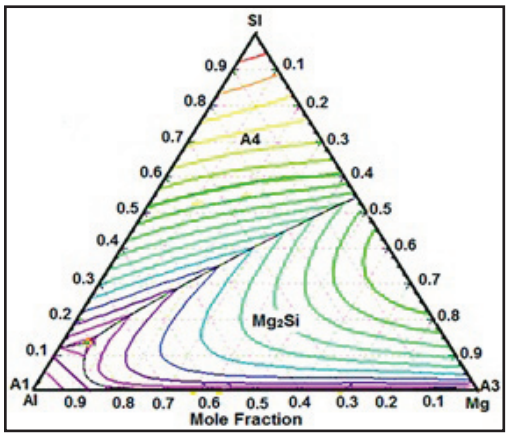

Fig. 17: Al-Si-Mg Phase Diagram

As shown in Al-Mg phase diagram (fig. 16), the maximum solubility of Mg in Al is 17.4%. As per the binary phase diagram of Al-Mg, the strengthening precipitates could be α, β ($A_{l3}Mg_2$) and γ ($Al_{12}Mg_{17}$) phases. As 5050 Al alloy consists of considerable amount of Si, there is a possibility of Al-Si-Mg ternary phase diagrams. From the Al-Si-Mg ternary phase diagram (fig. 17), the probable strengthening precipitate could be Mg2Si. Also, the condensation of surplus vacancies into dislocation loops helps the nucleation Si clusters. Diamond structure (A4) is formed from Si precipitates without intermediate stages from the Si clusters. Figure 18 reveals the formation of strengthening precipitates in 5050 Al alloy. The β phase was present in the three studied samples. The γ phase was noticed in the 5050 Al alloy consisting of 0.30% Mg. An increase in the composite strength can also be attributed to the precipitate strengthening.

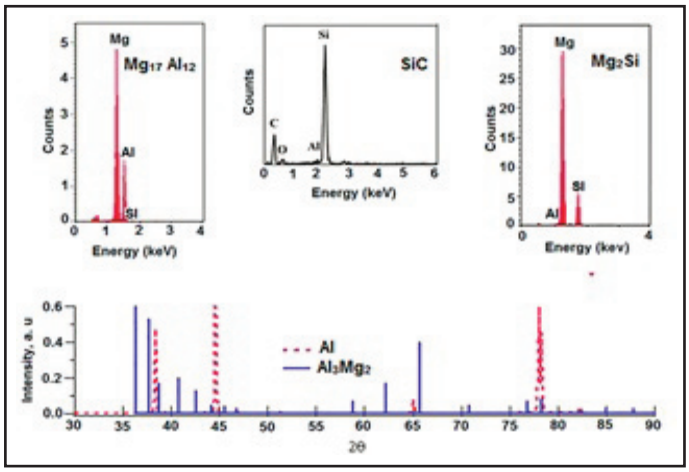

Fig. 18: Formation of Precipitates in SiC/5050 Al Alloy Composites

C. Schemes for Composite Stiffness

Modulus of elasticity is the measure of stiffness of a material. Einstein [31] proposed the stiffness of particulate composites based on the rigid particle assumption as follows:

$$\frac{E_c}{E_m} = 1 + 2.5v_p \qquad (8)$$

where Ec and Em are elastic modulus of composite and matrix, and Vp is nanoparticle volume fraction. Einstein's equation for the elastic modulus of particulate composites relays on assumption of uniform dispersion of reinforcement nanoparticles without interface between matrix and reinforcement. As observed from figure 4, the SiC nanoparticles are not dispersed uniformly in the matrix material of 5050 Al alloy. Hence, the predicted modulus of elasticity was diverged from the experimental value (figure 19). Another researcher, Kerner [32] estimated the modulus of elasticity of the composites assuming the spherical particles in a matrix as given below:

$$\frac{E_c}{E_m} = 1 + \frac{v_p}{(1-v_p)} \times \frac{15(1-v_m)}{(8-10v_m)} \qquad (9)$$

The clusters of SiC nanoparticles were formed; the clusters were not spherical in shape. Hence, the projected values of the elastic modulus are much lower than the experimental values as shown in figure 19. For a two-phase particulate composite, Counto [33] computed the modulus of elasticity assuming the perfect bonding between filler and matrix as stated below:

$$\frac{1}{E_c} = \frac{1-v_p^{1/2}}{E_m} + \frac{1}{(1-v_p^{1/2})/v_p^{1/2}E_m + E_p} \qquad (10)$$

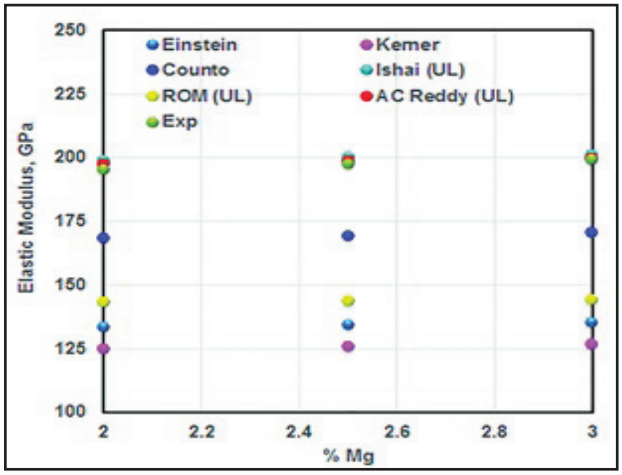

Fig. 19: Elastic Modulus of SiC/5050 Al Alloy Composites as a Function of Mg Content.

As per the wettability analysis of SiC/5050 Al alloy composites, a partial bonding was observed between the SiC nanoparticlas and the matrix alloy. Also, the SiC/5050 Al alloy composite did not a two-phase particulate composite according EDS analysis wherein the formation of precipitates were observed. Hence, the computed modulus of elasticity was lower than the experimental value. Ishai and Cohen [34] estimated the modulus of elasticity assuming perfect adhesive bonding at the interface between particulate and matrix with a state of macroscopically homogeneous stress field as given below:

$$\frac{E_c}{E_m} = 1 + \frac{1+(\delta-1)v_p^{2/3}}{1+(\delta-1)(v_p^{2/3}-v_p)} \qquad (11)$$

$$\delta = E_p / E_m$$

The predicted values were slightly higher than the experimental values due to the presence of voids and imperfect bonding. The scheme proposed by AC Reddy [29-30] to find the elastic modulus of composites including perfect boding, interphase between particles and matrix, formation of clusters and effect of voids/ porosity is given below:

$$\frac{E_c}{E_m} = \frac{1-v_p^{2/3}}{1-v_p^{2/3}+v_v} + \frac{1+(\delta-1)v_p^{2/3}}{1+(\delta-1)(v_p^{2/3}-v_v)} \qquad (12)$$

The predicted values of elastic modulus using Eq. (12) would match with the experimental data with very small deviation owing to the kind of bonding between SiC nanoparticles and matrix.

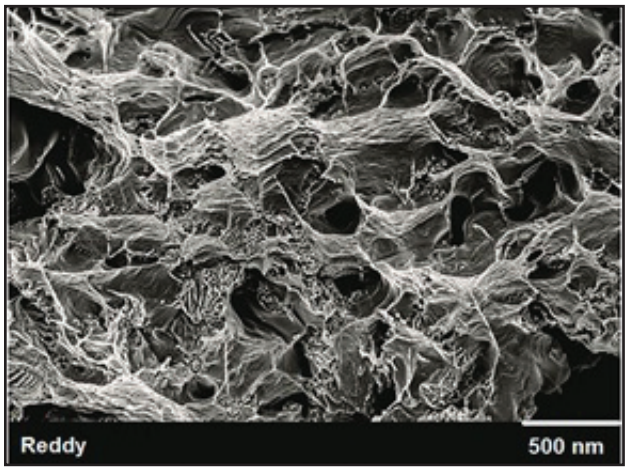

Fig. 20: Fracture Surface of SiC/5050 Al Alloy Composites

D. Fracture Behavior

Particulate reinforced metal matrix composites are isotropic and their fracture behavior is similar to that of conventional alloys. The SiC nanoparticles are stiffer and harder than the matrix 5050 Al alloy. The matrix alloy bears the major portion of the applied load. The SiC nanoparticles tend to restrain movement of the matrix (5050 Al alloy) phase in the vicinity of each nanoparticle. The presence of nanoparticles inhibits grain growth and high dislocation density. As read from the literature, the dominant mechanism of tensile failure in aluminum/silicon carbide systems is by void formation [35]. The fracture surfaces were nearly similar for the three SiC/5050 Al alloy composites comprising of 0.20%, 0.25% and 0.30% Mg content. The tensile fracture surface of SiC nanoparticles reinforced 5050 Al alloy shows a little evidence of voiding around SiC nanoparticles as shown in fig. 18. The fracture surface reveals shallow and long dimples. It is also observed that the interfacial sliding is lower than grain boundary sliding. The intermetallic phases were ruptured during the plastic deformation of tensile testing. These ruptured phases act as void nucleation sites. The other factors influencing fracture behavior are the non-uniform distribution of SiC nanoparticles and the formation of precipitates along the grain boundaries. Further, fig. 18 reveals the decohesion of nanoparticles from the matrix and cluster cracking.

IV. Conclusion

This research work was aimed at to investigate the influence of Mg addition in 5050 Al alloy used for the matrix material. The addition of Mg upto 3% could improve the wettability of 5050 Al alloy with SiC nanoparticles. When the magnesium content was increased beyond 3.0% in 5050 Al alloy, formation MgO precipitates were observed. For SiC/5050 Al alloy composites, the strengthening precipitates could be α, β (Al_3Mg_2), γ ($Al_{12}Mg_{17}$) and Mg2Si phases. The tensile strength and modulus of elasticity were enhanced due to increased content of Mg upto 3.0%. In the SiC/5050 Al alloy composites, the grain boundary sliding was dominating feature than the interfacial sliding resulting shallow and long dimples. The deviation experimental results with theoretical ones was attributed to imperfect bonding between SiC nanoparticle and matrix 5050 Al alloy.

VII. Acknowledgements

The authors thanks University Grants Commission (UGC), New Delhi for sponsoring this project.

References

[1] Reddy, A. C., Kotiveerchari, B., Rami Reddy, P.,"Saving of Thermal Energy in Air-Gap Insulated Pistons Using Different Composite Materials for Crowns," International Journal of Scientific & Engineering Research, Vol. 6, No. 3, pp. 71-74, 2015.

[2] Reddy, A. C.,"Influence of strain rate and temperature on superplastic behavior of sinter forged Al6061/SiC metal matrix composites," International Journal of Engineering Research & Technology, Vol. 4, No. 2, pp. 189-198, 2011.

[3] Reddy, A. C.,"Influence of Particle Size, Precipitates, Particle Cracking, Porosity and Clustering of Particles on Tensile Strength of 6061/SiCp Metal Matrix Composites and Validation Using FEA," International Journal of Material Sciences and Manufacturing Engineering, Vol. 42, No. 1, pp. 1176-1186, 2015.

[4] Reddy, A. C.,"Influence of Interphase on Tensile Behavior of Strain Hardened AA1100/AlN Nanocomposites Using RVE Models and Experimental Validation," International Journal of Engineering, Science and Technology, Vol. 7, No. 7, pp. 239-250, 2015.

[5] Alavala, C. R.,"Micromechanics of Thermoelastic Behavior of AA2024/MgO Metal Matrix Composites," International Journal of Advanced Technology in Engineering and Science, Vol. 4, No. 1, pp. 33-40, 2016.

[6] Reddy, A. C.,"Effects of Adhesive and Interphase Characteristics Between Matrix and Reinforced Nanoparticle of AA3105/AlN Nanocomposites," International Journal of Mechanical Engineering, Vol. 4, No. 5, pp. 25-36, 2015.

[7] Alavala, C. R.,"Tribological Investigation of the Effects of Particle Volume Fraction, Applied Load and Sliding Distance on AA4015/Titania Nanocomposites," IPASJ International Journal of Mechanical Engineering, Vol. 4, No. 10, pp. 9-15, 2016.

[8] Alavala, C. R.,"Nanomodeling of nonlinear thermoelastic behavior of AA5454/silicon nitride nanoparticulate metal matrix composites," International Journal of Engineering Research and Application, Vol. 6, No. 1, pp. 104-109, 2016.

[9] Alavala, C. R.,"Micromechanics of Thermoelastic Behavior of AA6070 Alloy/Zirconium Oxide Nanoparticle Metal Matrix Composites," International Journal of Engineering Research & Science, Vol. 2, No. 2, pp. 1-8, 2016.

[10] Alavala, C. R.,"Micromechanical Modelling of Thermoelastic Behavior of AA7020/TiC Metal Matrix Composites," International Journal of Scientific Engineering and Research, Vol. 4, No. 2, pp. 1-5, 2016.

[11] Reddy, A. C.,"Effects of Adhesive and Interphase Characteristics between Matrix and Reinforced Nanoparticle of AA8090/AlN Nanocomposites," Asian journal of engineering and technology, Vol. 3, No. 5, pp. 505-511, 2015,

[12] Canul, M. I. P., Katz, R.N., Makhlouf, M.M.,"The role of silicon in wetting and pressureless infiltration of SiCp preforms by aluminum alloys," Journal of Materials Science, Vol. 35, pp. 2167–2173, 2000.

[13] Ren, S., Shen, X., Qu, X., He, X.,"Effect of Mg and Si on infiltration behavior of Al alloys pressureless infiltration into porous SiCp preforms," International Journal of Minerals, Metallurgy and Materials, Vol. 18, No. 6, pp. 703–708, 2011.

[14] Sobczak, N., Ksiazek, M., Radziwill, W., Morgiel, J., Baliga, W., Stobierski, L.,"Effect of titanium on wettability and interfaces in the Al/ SiC system," Proceedings International Conference High Temperature Capillarity, Cracow, Poland, 29 June–2 July 1997.

[15] Reddy, A. C.,"Estimation of Thermoelastic Behavior of Three-phase: AA1100/Ni-Coated Boron Carbide Nanoparticle Metal Matrix Composites," International Journal of Scientific & Engineering Research, Vol. 6, No. 10, pp. 662-667, 2015.

[16] Zakaria, H. M.,"Microstructural and corrosion behavior of Al/SiC metal matrix composites," Ain Shams Engineering Journal, Vol. 5, pp. 831–838, 2014.

[17] Kiourtsidis, G. E., Skolianos, S. M., "Stress Corrosion Behavior of Aluminum Alloy 2024/Silicon Carbide Particles (SiCp) Metal Matrix Composites," Vol. 56, No. 6, pp. 646-653, 2000.

[18] Reddy, A. C.,"Tensile properties and fracture behavior of 6063/SiCP metal matrix composites fabricated by investment casting process," International Journal of Mechanical Engineering and Materials Sciences, Vol. 3, No. 1, pp. 73-78, 2010.
[19] Reddy, A. C.,"Influence of volume fraction, size, cracking, clustering of particulates and porosity on the strength and stiffness of 6063/SiCp metal matrix composites," International Journal of Research in Engineering and Technology, Vol. 4, No. 1, pp. 434-442, 2015.
[20] Reddy, A. C.,"Tensile fracture behavior of 7072/SiCp metal matrix composites fabricated by gravity die casting process," Materials Technology: Advanced Performance Materials, Vol. 26, No. 5, pp. 257-262, 2011.
[21] Reddy, A. C.,"Studies on loading, cracking and clustering of particulates on the strength and stiffness of 7020/SiCp metal matrix composites," International Journal of Metallurgical & Materials Science and Engineering, Vol. 5, No. 1, pp. 53-66, 2015.
[22] Bowen, A. W., Humphreys, F. J.,"Texture Development in Hot-Rolled 8090 Aluminium Alloy-SiC Metal-Matrix Composites," Textures and Microstructures, Vol. 14-18, pp. 715-720, 1991.
[23] Bai, L., Xiujuan, L., Mingjun, L., Zhenyu Z.,"Infiltration Mechanism in SiCp/Aluminum-Matrix Composite Prepared by Nonpressure," Vol. 26, No. 11, pp. 1339-1345, 2011.
[24] Adamson A. W., Physical Chemistry of Surfaces, J. Wiley & Sons, New York 5th edition, 1990.
[25] Pukanski, B., Fekete, E.,"Adhesion and surface modification," Advances in Polymer Science, Vol. 139, pp. 109–153, 1999.
[26] Fu, S. Y., Feng, X. Q., Lauke, B., Mai, Y. W.,"Effects of particle size, particle/matrix interface adhesion and particle loading on mechanical properties of particulate-polymer composites," Composites B, Vol. 39, No. 6, pp. 933–961, 2008.
[27] Pukanszky, B., Turcsanyi, B., Tudos, F.,"Effect of interfacial interaction on the tensile yield stress of polymer composites. In: Ishida H, editor. Interfaces in polymer," Ceramic and metal matrix composites. Amsterdam: Elsevier, 1988, pp. 467–477.
[28] Hojo, H., Toyoshima, W., Tamura, M., Kawamura, N., "Short- and longterm strength characteristics of particulate-filled cast epoxy resin," Polymer Engineering & Science, Vol. 14, pp. 604–609, 1974.
[29] Reddy, A. C.,"Effects of Adhesive and Interphase Characteristics between Matrix and Reinforced Nanoparticle of AA5154/AlN Nanocomposites," International Journal of Advanced Research, Vol. 3, No. 9, pp. 703-710, 2015.
[30] Reddy, A. C.,"Cause and Catastrophe of Strengthening Mechanisms in 6063/Al_2O_3 Composites Prepared by Stir Casting Process: Validation through FEA," International Journal of Scientific & Engineering Research, Vol. 6, No. 3, pp. 75-83, 2015.
[31] Einstein, A.,"Ueber die von der molekularkinetischen fluessigkeiten suspendierten teilchen," Annals of Physics (Leipzig), Vol. 17, pp. 549–560, 1905.
[32] Kerner, E.H.,"The Elastic and Thermo-Elastic Properties of Composite Media," Proceedings the Physical Society, London, Vol. B69, pp. 808, 1956.
[33] Counto, U. J.,"Effect of the elastic modulus, creep and creep recovery of concrete," Magazine Concrete Research, Vol. 16, pp. 129–38, 1964.
[34] Isha, O., Cohen, I. J.,"Elastic properties of filled and porous epoxy composites," International Journal of Mechanical sciences, Vol. 9, pp. 539–546, 1967.
[35] Humphreys, F J.,"Mechanical and physical behaviour of metallic and ceramic composites," (Eds S I Andersen et al) Riso National Laboratory, pp. 51, 1988.

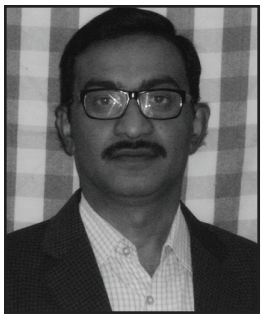

Dr. A. Chennakesava Reddy, B.E., M.E (prod)., M.Tech (CAD/CAM)., Ph.D (prod)., Ph.D (CAD/CAM) is a Professor in Mechanical Engineering, Jawaharlal Nehru Technological University, Hyderabad. The author has published 534 technical papers worldwide. He is the recipient of best paper awards eleven times. He is recipient of Best Teacher Award from the Telangana State, India. He has successfully completed several R&D and consultancy projects. He has guided 18 Research Scholars for their Ph.D. He is a Governing Body Member for several Engineering Colleges in Telangana. He is also editorial member of Journal of Manufacturing Engineering. He is author of books namely: FEA, Computer Graphics, CAD/CAM, Fuzzy Logic and Neural Networks and Instrumentation and Controls. Number of citations are 6013. The h and i10 indices are 44 and 165, respectively. The His research interests include Fuzzy Logic, Neural Networks, Genetic Algorithms, Finite Element Methods, CAD/CAM, Robotics and Characterization of Composite Materials and Manufacturing Technologies.